I Nevares, T Mayr, JA Baro, J Ehgartner, R Crespo, M del Alamo-Sanza.
Ratiometric Oxygen Imaging to Predict Oxygen Diffusivity in Oak Wood During Red Wine Barrel Aging.
Food and Bioprocess Technology June 2016, Volume 9, Issue 6, pp 1049–1059

Ratiometric oxygen imaging to predict oxygen diffusivity in oak wood during red wine barrel aging

Ignacio Nevares [a], *Torsten Mayr* [b], *Jesús Ángel Baró* [a], *Josef Ehgartner* [b], *Raúl Crespo* [a], *María del Álamo-Sanza* [a*]

[a] Grupo UVaMOX, E.T.S. Ingenierías Agrarias, Universidad de Valladolid, 34004, Palencia, Spain
[b] Applied Sensors, Institute of Analytical Chemistry and Food Chemistry, Graz University of Technology, 8010 Graz, Austria.
*delalamo@qa.uva.es

INTRODUCTION

The oxidation of wine during storage in oak barrels is a well-known fact and is recognized as an important process in wine aging. Work by Vivas *et al.* [1] and work recently published by our team [2,3] support the idea that oxygen transmission to wine occurs not only through gaps between the oak pieces of a barrel, but it also permeates the oak wood, which remains permeable to oxygen even after several months in contact with wine. The oxygen transmission rate (OTR) to the wine has been measured as a dynamic rate for one year [4]. Because of the contact time between the wine and wood, the moisture content (MC) of the oak wood increases and, more specifically, the presence of free water in the wood correlates well with the decrease of the OTR over time.

In previous work from our research group, we confirmed that variations in the OTRs of the wood staves of wine barrels in contact with liquid significantly affect the transmission of atmospheric oxygen to the liquid inside the barrel (del Alamo-Sanza and Nevares 2014). According to the work of Feuillat (Feuillat 1996) and Ruiz de Adana (S. M. Ruiz de Adana 2002), the impregnation front of a stave in equilibrium is 4–5 mm thick. Therefore, the rest of the wood does not reach the FSP but rather exhibits varying water content in a hygroscopic form. The saturated part of the inner face of the stave in contact with the liquid, which includes the wood affected by the toasting process, contains water in the free form.

Fick's first law can be considered as a specific (simplified) form of the second law when applied to a steady state, where the concentration remains constant.

$$J = -D \cdot \frac{dc(x)}{dx} \quad (1)$$

Here, J is the "diffusion flux," which measures the amount of a substance that will flow through a small area during a small time interval ($mol \cdot m^{-2} \cdot s^{-1}$); D is the diffusion coefficient or diffusivity ($m^2 \cdot s^{-1}$); c is the concentration in the direction of the flux ($mol \cdot m^{-3}$); and dx is position (m).

The diffusion of a gas through a membrane whose properties change with thickness is a special case of diffusion resembling that through a membrane composed of layers with

differing thicknesses and diffusion coefficients. The mathematical treatment of the non-stationary state is complicated, but if the permeable gas is considered stable, the case can be treated more easily. Let n films with thicknesses $x_1, x_2, \ldots, x_n$ with their corresponding coefficients of diffusion $D_1, D_2, \ldots, D_n$ be considered as a multilayer membrane. Under these conditions, for a multi-layered system with n layers, a series-resistance model (SRM; often called the ideal laminate theory) is often used to produce the following steady-state flux equation (Equation 2) (Graff et al. 2004). This approximation has been previously used for wood by other authors (Huang et al. 1977). Since, in steady state, the flow J of a substance that diffuses i is the same through each individual component of the laminate, the following expression is obtained for the concentration gradient (Piringer and Baner 2000):

$$\Delta c = \frac{J \cdot x_1}{D_1} + \frac{J \cdot x_2}{D_2} + .. + \frac{J \cdot x_n}{D_n} = J \cdot \left(\frac{x_1}{D_1} + \frac{x_2}{D_2} + .. + \frac{x_n}{D_n}\right) \quad (2)$$

with the resistance $R_1 = x_1 / D_1$, etc.

The total resistance related to diffusion is then the sum of the individual resistances, and the total flux is practically determined by the layer with the smallest diffusion coefficient (Piringer and Baner 2000). In our case, the thickness of a wood stave can be approximated as a multilayer system whose layers are differentiated by water content.

$$J = \frac{\Delta c1}{\frac{x_1}{D_1}} = \frac{\Delta c2}{\frac{x_2}{D_2}} = \frac{\Delta c3}{\frac{x_3}{D_3}} = \cdots = \frac{\Delta cn}{\frac{x_n}{D_n}} \quad (3)$$

Here, the subscripts 1, 2, . . ., n denote the layer number, with 1 being the downstream inlet side of the stave and n the upstream outlet side. To understand permeation through a multilayer stack, it is necessary to know the diffusion coefficient or diffusivity of each constituent layer, which in this case depends on the water/air oxygen diffusivity. Moreover, according to this approximation, the limiting layer of a stave is equivalent to that of wood flooded with water, for which the diffusivity is in the same order of magnitude that of oxygen in water; this diffusivity is much lower than oxygen diffusivity in air. Because the remaining wood layers do not reach the FSP and the water is in the hygroscopic form, the OTR depends on the oxygen solubility in the air. Therefore, the OTR will reach its minimum value when the impregnation front reaches a maximum (Hicks and Harmon 2002), which, according to the work of Feuillat (Feuillat 1996), will occur 82 days after the filling of the barrel, when the front will exhibit a 4–5 mm thickness (S. M. Ruiz de Adana 2002).

These results reveal the importance of the level of wood impregnation to the OTR. It was deemed appropriate to use a system approximating a barrel scenario (liquid-wood-air). This setup (Del Alamo and Nevares 2012) was therefore used in this work to evaluate the OTR in barrels. In the work of Vivas *et al.* (Vivas et al. 2003), a gas-wood-gas system was used according to the guidelines established for assays of membrane permeability. This setup did

not reproduce the actual situation of staves in a barrel, as the impregnation effect was not considered.

Image analysis techniques for the determination of dissolved oxygen have been employed in different formats by using sensitive luminescent dyes (Mehta et al. 2007; Sud et al. 2006), sensor beads (Ungerböck et al. 2013) or sensor layers (Nevares et al. 2014). In addition, different reading systems have been used in imaging configurations applied to biological material. Intensity imaging can be implemented easily, but it has the disadvantage of undesirable signal variations due to defects in the optical system, such as heterogeneity in the light source, non-homogeneous sensitivity in the detection system or a non-homogeneous distribution of fluorescent sensors in the detection matrix. These problems limit the accuracy of the oxygen images obtained (Ungerbock et al. 2013; Ungerböck et al. 2010). Fluorescence lifetime imaging, on the other hand, gives very accurate results but requires expensive and specialized instrumentation, thus limiting its application (Liebsch et al. 2000). This work, therefore, implements 2-wavelength ratiometric imaging to combine low cost with the use of readily available high-resolution equipment. A color CCD camera measures the intensity of the 2 different wavelengths of light emitted from the sensor by using different color channels of the camera. Image intensity that is sensitive to oxygen is provided by one channel, while the other provides a reference image. By calculating the relationship between these images (red image/green image), a ratiometric image is obtained that is independent of the inhomogeneities listed above.

The objective of this study was to apply ratiometric oxygen imaging to a stave of a wine barrel. This technology has been used in a trial, under conditions resembling those of the wood composing a barrel full of wine, to explore the variation in oxygen concentration inside the stave and thus corroborate the established hypothesis. In this hypothesis, the advance of free water in the wood stave in a direction that is opposite to the flow of oxygen entry is responsible for the decrease in oxygen diffusivity (Nevares et al. 2014). It can thus explain the decrease in the OTR of barrel wood when the wine is aged.

1) MATERIALS AND METHODS

The need to know the distribution of MC in combination with the OTR and the variation in oxygen concentration inside a stave, across the entire thickness of the stave and at different times during wine aging, has made the application of 3 very different techniques essential. As one is destructive, 3 simultaneous assays have been developed.

Studied wood

A stave extracted from a barrel made with medium roast French oak (*Quercus petraea*) from the Center forests was used. A homogeneous stave with a uniform distribution of rings both

in its form and width was chosen to minimize the variability in the actual morphological structure of the natural material. From the selected stave, test specimens (Figure 1) measuring 40 mm in diameter by 29 mm in thickness were extracted.

→Figure 1:

Wood for measurement of OTR and the moisture profile of the stave. Measurement of OTR was performed in conditions resembling those of a stave in a barrel full of liquid and at different times of the aging process (0, 6, 13, 20, 63, 88 and 125 days), following the protocol described in a previous study (Nevares and del Alamo-Sanza 2015). The different specimens were conditioned in contact with a sterilized model wine (14% v/v EtOH, pH 3.5) under hydrostatic pressure conditions resembling those of a stave halfway up the barrel, and they thus reached states of wood moisture that were characteristic of each test period. Once the OTR trial was conducted, the piece of wood was laminated to determine the distribution of moisture throughout the entire thickness of the stave. It is important to note that the OTR-moisture measurements were taken on different samples, as they are destroyed during each measurement; however, as we used contiguous samples from the same homogeneous stave, the samples are assumed to have very similar properties.

Wood for image analysis. A piece of wood contiguous to those used in the OTR measurement was extracted and placed in a device developed in a previous study (Nevares et al. 2014) to evaluate the level of dissolved oxygen (DO) inside the stave during the aging of red wine. We used red wine that was obtained from the Tempranillo variety and had a pH of 3.39, total acidity 4.5 $g.L^{-1}$, volatile acidity 0.52 $g.L^{-1}$ and an alcohol content of 13.81% (v/v). The use of wine is particularly relevant, as the rapid consumption of oxygen by the wine ensures a DO concentration gradient (driving force of oxygen entry by diffusion) that is essential for evaluation of the DO distribution inside the stave.

Measurement of moisture distribution in the thickness of the stave

The moisture gradient in the wood is not easy to measure nondestructively, as moisture is associated with many other properties of wood, such as density and temperature (Gu and Zink-Sharp 1999). The most common method for measuring the moisture gradient of wood is the band saw-based laminate technique described elsewhere (Mcmillen 1955). However, besides being destructive, this traditional technique generates errors from moisture loss that occurs when cutting each sheet (especially when the temperature is high), from incorrect weighing caused by the sensitivity of the thin layers of wood to low humidity, or from loss of wood in the teeth of the saw that cuts each sheet. When the laminate is made with a blade, it has a reduced effect on the moisture content of the sheets that are produced (Gorvud and Arganbrigh 1980). This study used a device that was developed based on a commercial horizontal wood slicer to laminate each wood specimen into sheets with thicknesses between 0.5 mm and 2 mm. Subsequently, the moisture content of each sheet was determined using

the dry weight method (ASTM 2009). A well-performed measurement allows for an uncertainty between 0.3% and 1.4% (Rosenkilde 2002).

Measurement of DO inside the wood

To determine the level of DO inside the stave, we used a device that was developed and used in a previous study (Nevares et al. 2014). The system basically consists of a container with a transparent side, in which a planar photoluminescent sensor and a piece of stave are fixed in such a way that a cross section of a stave in a full barrel is reproduced. Thus, the wood is in contact with air on one side and with wine on the other side. The container has a system that reproduces the normal pressure inside a barrel (Peterson 1976).
We used ratiometric imaging that employed the red and the green channels of a color CCD camera as shown by Ungerböck et al. 2010 and Larsen et al. 2011. We used an alternative indicator dye (Pd-porphyrin) to achieve trace oxygen concentration measurement. The spectral properties are virtually the same. The oxygen-sensitive emission of sensor foils was detected in the red channel, while the emission of a reference dye was detected in the green channel. This measurement setup allowed for accurate, real-time 2-dimensional (2D) oxygen imaging with superior quality compared to intensity imaging.

Sensor foils were prepared with a sensor cocktail for O_2 measurements. Melinex 506 (thickness 125 μm) was used as a substrate for the sensor foils. A sensor cocktail containing palladium(II)-5,10,15,20-tetrakis-(2,3,4,5,6-pentafluorphenyl)-porphyrin (PdTPFPP, 3.6 mg), Macrolex Fluorescence Yellow (MFY, 5.9 mg) and polystyrene (PS, M = 250,000, 300 mg) in chloroform (4.4 g) was knife-coated (BYK Drawdown Bar 3 Mil) on the substrate foil. After drying the sensor foil at 60°C, some sensor foils were additionally knife-coated (BYK Drawdown Bar 3 Mil) with a protection cocktail, which contained ELASTOSIL® E4 silicon rubber (1 g) in hexane (3 g).

Macroscopic oxygen imaging was performed using a 458 nm high-power 10 W LED array (www.led-tech.de) as excitation source. The filter set consisting of an excitation filter BG12 (350–470 nm) and a long-pass emission filter OG515 (515 nm) was purchased from Schott (www.schott.com). An AVT Marlin F-201C color camera equipped with a Pentax TV Lens 12 mm f/1.2 C-mount lens (http://www.schneiderkreuznach.com) was used for image acquisition. The camera uses the Sony ICX 285 AQ image sensor. Image acquisition was performed with the software AVT SmartView (http://www.alliedvisiontec.com). Matlab R2009a (www.mathworks.com) was used for image processing. The color channels of the obtained images were separated and the ratiometric image R was obtained by dividing the red by the green channel. Fitting was performed using OriginLab 8.6 (www.originlab.com).

Sensor foils calibration. The sensors (PdTPFPP/MFY) were gas-phase calibrated in a home-made calibration chamber. Two mass flow controller instruments (Read Y smart series) by

Vögtlin instruments (www.voegtlin.com) were used to obtain gas mixtures of defined pO2. Compressed air and nitrogen or 2 % (v/v) oxygen in nitrogen and nitrogen were used as calibration gases. The exact oxygen concentrations within the calibration vessel were determined with an optical oxygen meter (FireStingO2) from Pyroscience connected to a fiber-optic oxygen sensor (www.pyro-science.com).

Image analysis. Acquired images were split into the red, green, and blue channels and were analyzed using C routines and the OpenCV library (Itseez (2015) Open Source Computer Vision Library, https://github.com/itseez/opencv) to obtain 50%-truncated, or interquartile, means of the color channel values at each column of pixels. These columns were set parallel to the wood-wine interface.

Measurement of OTR in wood pieces

The OTR measurement method developed by our research group and used in previous studies was used (Nevares and del Alamo-Sanza 2015), and then, the necessary calculations to estimate diffusion flux ($mol \cdot m^{-2} \cdot s^{-1}$) were made, following the studies of Sorz and Nietz (Sorz and Hietz 2006). The device dimensions maintain the same wood surface/liquid volume ratio as a 225-L Bordeaux barrel. The hydrostatic pressure of the liquid in contact with the stave was matched to the pressure of a stave halfway up the barrel, see (Nevares and del Alamo-Sanza 2015) for a full description of the device. Each of the different times of the process (0, 6, 13, 20, 32, 63, 88 and 125 days) were subject to measurement of OTR, and the moisture distribution inside the specimen was subsequently measured using the previously described method.

2) RESULTS AND DISCUSSION

According to Fick's first law, the flow of oxygen J that crosses the wood of the stave from the outside to the inside of the barrel varies as a function of wood-liquid contact time. This flow is a direct function of the diffusion coefficient of wood and the oxygen concentration gradient at both sides of the stave wood thickness (Equation 1). To test this relationship, three parallel experiments were conducted that provided the necessary data at different times during the aging process (0, 6, 13, 20, 32, 63, 88 and 125 days). On one side, with test A, the flow of oxygen that crosses the wood J ($mol \cdot m^{-2} \cdot s^{-1}$) was measured. In test B, the MC inside the stave (% MC) was obtained at each of the times, and, more importantly, we obtained the distribution of this MC within the thickness of the stave and therefore determined the thickness of wood e with a % MC > FSP. In test C, by ratiometric analysis of the images acquired with a camera, an oxygen concentration profile within the wood was obtained, allowing us to determine the gradient of concentrations Δc along the thicknesses e of the stave obtained in test B.

Sensor foils calibration. Figure 2a shows a calibration of a sensor foil with mixtures of compressed air and N2 and figure 2b shows a calibration of the same foil with mixtures of 2 % O2 in N2 and N2 (purity of 5.0). Referenced images can be seen in figure 2c and 2d.

→Figure 2:

The distribution of moisture throughout the thickness of the stave at 7 times of wood-synthetic wine contact (all but time 0), obtained using the slicing method, revealed how aging time determinately influences the % MC of wood. As shown in Figure 3, after the first week, free water appears in the first mm of wood in contact with wine. As time progresses, the % MC of the wood progressively increases, so that at the end of the test period (4 months), free water is present in the first 10 mm of thickness of the stave from the face in contact with wine (Table 1). In this regard, no currently published studies have reported this water penetration depth, as data from previous studies (del Alamo-Sanza and Nevares 2014; Nevares et al. 2014) estimated this value to be approximately 4-5 mm of wood, although previous work did not clearly specify the levels of moisture in this flooded thickness. The Ruiz de Adana modeling estimated that this level stands at 6 mm (M. Ruiz de Adana et al. 2005); confirming the experimental data of Feuillat (Feuillat 1996), where, in the initial stage of wood-wine contact, the rate of advance of the impregnation front is a linear function of the square root of the contact time. If we consider the wood to be flooded above % MC = 60%, our data would coincide fully with the results published by other authors (Feuillat 1996; S. M. Ruiz de Adana 2002). The trend that moisture content progressively increases over time confirms the results of previous studies (del Alamo-Sanza and Nevares 2014; Nevares et al. 2014).

→Figure 3:

When we measured the oxygen transfer rate of wood at different times of contact with the wine, the same trend described in previous studies was found (del Alamo-Sanza and Nevares 2014), in which the value progressively changed over time. In the present study, the diffusion flux J, calculated using the OTR data from test A, followed the trend $J = 3 \times 10^{-5} \cdot t^{-1.929}$ ($R^2 = 0.9285$, Figure 4), where J is expressed as $mol \cdot m^{-2} \cdot s^{-1}$ and aging time (t) in days . Thus, the MC of the wood, which progresses similarly but in the opposite direction of the flow of oxygen diffusion, may be responsible for the decrease in oxygen diffusion flux as contact time increases. To prove this notion, we propose applying the concept of the series-resistance model, where the flow of diffusion is defined by the wood layer in which the resistance to the flow of oxygen is greatest. As described in Equation 3, the portion of the wood thickness (e) that contains free water (% MC > FSP) was considered as the wood layer with the greatest resistance to the flow of oxygen.

→Figure 4:

→Table 1

In test C, the image capture of the planar sensor with the CCD camera and its subsequent ratiometric analysis were used to identify the average oxygen concentration in each layer of wood at different distances from the surface in contact with the red wine (figure 5).

→Figure 5.

Table 1 shows the oxygen concentration gradient ($mol \cdot m^{-3}$) at each side of the wood layer, along with free water (*e*: thickness MC > FSP (m)), at each time during aging. Figure 6 shows the progression of the oxygen concentration profile within the stave at each of the studied times; the black vertical line at 18.3 mm in the captured image represents the wood-wine limit. In the layers of wood closest to the wine (from a 15-mm distance from the sensor foil to the limit of the wine), the oxygen concentration was shown to significantly decrease, at the same time producing an accumulation of oxygen inside the wood. This accumulation increases over time and is closely related to the advance of the free water front in the wood. During the preparation of test C, and as a result of the degassing process of the wine chamber, the wood was also degassed. When the space within the wood becomes filled with wine that has very low levels of DO (2-3% air sat.), it can be seen how the wine contains more oxygen than the wood (t = 0 days). However, as the contact time increases, the wine consumes its own dissolved oxygen, along with all the oxygen from the outside that enters the wine through the wood. Simultaneously, where the wine penetrates the wood, there is a drop in the oxygen level due to its rapid consumption by the wine. An air/wine interface (at 18.3 mm) was observed (t = 6 and 13 days), in which a higher level of DO was present than in the rest of the wine due to the flow of oxygen from the wood. With the passage of time and as the wine penetrated the wood, the flow of oxygen entry significantly decreased (Table 1), and the interface revealed how the high rate of oxygen consumption maintains a very low DO concentration in the wine. The oxygen levels in the wood were higher in the layers closest to the outside, and they increased over time due to the decrease in diffusion flux. At 13 days, we had already observed a notable jump in the oxygen concentrations that was caused by the slowdown in the oxygen transfer of wood. In the following time points (20 and 32 days), this oxygen concentration gradient was displaced towards the interior of the stave, resembling the displacement of the moisture front of the wood. That is, the free water front acts as a brake on the transfer of oxygen by the wood towards the wine, thereby causing the accumulation of oxygen inside the stave ($t \geq 13$). As the contact time with the wine increases, the oxygen concentration equalizes within the wine and the wood-wine limit, as the gradient has moved inside the stave. We observed that, at 2 months (63 days), the oxygen content within the wood increased, and an interface formed at a greater distance from the side of the stave in contact with the wine. Meanwhile, the wood, with its MC in the form of "free wine" (formally free water), reduces its oxygen concentration as it is consumed by the wine present in the wood. As the days continue to pass, the concentration of oxygen inside the flooded wood decreases considerably, and at 4 months (125 days), it becomes practically zero in the first 3 mm of the stave on the side that contacts the wine.

→Figure 6.

In Figure 7, the oxygen concentration (data from test C) and wood moisture (measured in test B) profiles are shown at 4 selected times. A relationship may be clearly seen between the thickness of the wood with a % MC above its FSP (see Table 1) and the formation of a jump in oxygen concentration. The oxygen concentration jump represents the accumulation of oxygen that occurs as a result of the lowered diffusion coefficient of wood due to the presence of free water. The jump in the level of DO is produced at the air-wine interface, and occurs as a result of the change in the oxygen diffusion coefficient of wood. A displacement of this interface toward the interior of the wood occurs, and it coincides very precisely with the MC front due to the existence of free liquid that is not bounded to the wood.

→Figure 7.

To test the hypothesis that moisture in the stave due to contact with wine affects the ability of wood to diffuse atmospheric oxygen, the diffusion coefficient was calculated with equation 1. For this purpose, at each of the 7 time points studied, the flow of oxygen diffusion J (mol·m^{-2}·s^{-1}) calculated from the measured OTR (test A) and the moisture profile within the stave (test B) were used. This profile allowed us to determine the thickness of the wood layer with a % MC higher than the FSP, that is, with free water present in its porosity, which has been postulated to act as a barrier to the diffusion of atmospheric oxygen in different media (Hansmann et al. 2002; Mugnai and Mancuso 2010; Rosenkilde 2002; Sorz and Hietz 2006). Additionally, thanks to the ratiometric analysis of the oxygen content inside the stave, the oxygen concentration gradient was obtained for the layer of wood with free water, which acts as a driving force for diffusion (test C). With these values that were obtained from the 3 parallel tests (shown in Table 1), it was then possible to determine the diffusion characteristics of wood with free water and its relationship with the free water content and the thickness of flooded wood (% MC > FSP).

Figure 4 shows the existing relationship between the diffusion flux, calculated with data from test A, and the thickness of wood with free water, obtained from test B, at the studied time points. Their relationship follows a potential line that was adjusted to the calculated data ($J = 6 \times 10^{-8} \cdot e^{-1.461}$; $R^2 = 0.8754$), where J is expressed as mol·m^{-2}·s^{-1} and e in mm. Once we confirmed that the data determined from the OTR calculations followed a potential equation over time, it was necessary to know whether this relationship was maintained when the diffusion coefficient D was calculated (Table 1) using the data from the 3 parallel tests (A: OTR, B: % MC profile and C: O_2 concentration profile). In Figure 8, the potential relationship ($D = 8 \times 10^{-7} \cdot e^{-1.797}$; $R^2 = 0.8609$) is shown, which follows the oxygen diffusion coefficients of staves that have different wood thicknesses with free water at the different times of contact with the wine.

→Figure 8.

The wood thickness containing free water clearly affects D, but to know in detail if, in addition to the wood thickness with free water, the level of free water has any influence on oxygen diffusion flux, a new variable was calculated (eMC) that is the product of the thickness e of the flooded layer (% MC > FSP) and of its average % MC, i.e., the average free water that exists in that thickness (Table 1) obtained from test B. In Figure 8, the existing relationship among the water content of the layer of thickness e with a % MC > FSP, the DO concentration gradient and the oxygen diffusion coefficient (D) calculated with the data obtained from the 3 tests is shown. Figure 8 shows that there is again a potential relationship ($D = 2 \cdot 10^{-5} \cdot e\mathrm{MC}^{-1.251}$; $R^2 = 0.927$) between the diffusivity of the layer, which acts as a brake to oxygen transfer (considering the theory of the serial resistance model and the thicknesses of the flooded layer), and its degree of flooding (% MC). Therefore, these results confirm what was described by Sorz and Hietz (Sorz and Hietz 2006) in a different situation, where the free water in oak wood significantly affected the diffusivity of oxygen, and they confirm previously published data (Mugnai and Mancuso 2010). It is evident how the diffusion coefficient D strongly increased with the volume of air, not only in the xylem in both axial and radial directions (Mugnai and Mancuso 2010), but also in the tangential direction, as in the case of an oak stave, which represents an atypical case (Hansmann et al. 2002).

3) CONCLUSIONS

The ratiometric image-analysis technique for quantifying DO through the use of developed sensors is a viable technique for determining the concentration gradients of dissolved oxygen within wood, as has already been demonstrated for other biological materials. The inflow of atmospheric oxygen towards the wine through the wood of the staves of the filled barrels is directly affected by wetting of the oak wood, which is mainly responsible for the slowdown in oxygen diffusion. The thickness of the layer of wood containing free water and its free water content are able to explain the decrease in the OTR of the wood from the staves of the barrels and allows for predicting the behavior of the diffusion coefficient that is ultimately responsible for oxygen diffusion flux. Therefore, because the impact of moisture on the diffusion coefficient is so dramatic, moisture is the most important factor leading to the very low OTR conditions in barrels just 2 months after filling. These results indicate a need to deepen our understanding of the roles played by botanical origin, cooperage treatments and the anatomy of wood in water diffusion, and hence in the progression of OTR in wood.

Funding

This work was financed by the Ministerio de Ciencia e Innovacion, Ministerio de Economía y Competitividad and the European Regional Development Fund (MICINN-FEDER,

AGL2011-26931 and MINECO-FEDER, AGL2014-54602-P) and by the Junta de Castilla y León (VA-086A11-2, VA124U14) from Spain.

References

ASTM. (2009). ASTM D1434 - 82(2009)e1 Standard Test Method for Determining Gas Permeability Characteristics of Plastic Film and Sheeting. West Conshohocken, PA: ASTM International. doi:DOI: 10.1520/D1434-82R09E01

Del Alamo, M., & Nevares, I. (2012). PCT/ES2012/070084 Device for measuring the permeability and diffusivity of gases in porous materials and method for measuring said parameters using the device. (W.-W. I. P. Organization, Ed.). PCT/ES2012/070084 International . http://patentscope.wipo.int/search/en/WO2012107625

del Alamo-Sanza, M., & Nevares, I. (2014). Recent Advances in the Evaluation of the Oxygen Transfer Rate in Oak Barrels. *Journal of Agricultural and Food Chemistry*, *62*(35), 8892–8899. doi:10.1021/jf502333d

Feuillat, F. (1996). Contribution à l'étude des phénomènes d'échanges bois/vin/atmosphère à l'aide d'un "fût" modèle. Relations avec l'anatomie du bois de chêne (*Quercus robur* L., *Quercus petraea* Liebl.). *Lab. de Recherches en Sciences Forestières de l'ENGREF*. Nancy; France: Ecole Nationale du Génie Rural des Eaux et des Forêts.

Gorvud, M. R., & Arganbrigh, D. G. (1980). Comparison of Methods for Preparation of Moisture Content Gradient Sections, *12*(1), 7–11. https://www.google.es/url?sa=t&rct=j&q=&esrc=s&source=web&cd=2&ved=0CCgQFjABahUKEwjmtOi_qq7IAhXIuBoKHf_6D4Y&url=http://wfs.swst.org/index.php/wfs/article/download/870/870&usg=AFQjCNEVhwzdeQpjbhnlqN2guCCQknO1qA&sig2=7oN4rLfBzh4laCKaXUhIWw

Graff, G. L., Williford, R. E., & Burrows, P. E. (2004). Mechanisms of vapor permeation through multilayer barrier films: Lag time versus equilibrium permeation. *Journal of Applied Physics*, *96*(4), 1840. doi:10.1063/1.1768610

Gu, H. M., & Zink-Sharp, A. (1999). Measurement of moisture gradients during kiln-drying. *Forest products journal*. http://agris.fao.org/agris-search/search.do?recordID=US201302915795. Accessed 6 October 2015

Hansmann, C., Gindl, W., & Wimmer, R. (2002). Permeability of wood - a review . *Wood research*, *47*(4), 1–16.

Hicks, W. T., & Harmon, M. E. (2002). Diffusion and seasonal dynamics of O2 in woody debris from the Pacific Northwest, USA. *Plant and Soil*, *243*(1), 67–79. doi:10.1023/a:1019906101359

Huang, H. I., Sarkanen, K. V, & Johanson, L. N. (1977). Diffusion of dissolved oxygen in liquid-saturated Douglas fir sapwood. *Wood Science and Technology*, *11*(3), 225–236. doi:10.1007/bf00365617

Larsen, M., Borisov, S. M., Grunwald, B., Klimant, I., & Glud, R. N. (2011). A simple and inexpensive high resolution color ratiometric planar optode imaging approach: application to oxygen and pH sensing. *Limnology and Oceanography: methods*, *9*(9), 348–360. doi:DOI 10:4319/lom.2011.9.348

Liebsch, G., Klimant, I., Frank, B., Holst, G., & Wolfbeis, O. S. (2000). Luminescence Lifetime Imaging of Oxygen, pH, and Carbon Dioxide Distribution Using Optical Sensors. *Applied Spectroscopy*, *54*(4), 548–559. http://www.osapublishing.org/abstract.cfm?uri=as-54-4-548. Accessed 22 October 2015

Mcmillen, J. M. (1955). Drying Stresses in Red Oak. *Forest Products Journal*, *5*(1), 71–76. http://www.fpl.fs.fed.us/documnts/pdf1955/mcmil55b.pdf

Mehta, G., Mehta, K., Sud, D., Song, J. W., Bersano-Begey, T., Futai, N., et al. (2007). Quantitative measurement and control of oxygen levels in microfluidic poly(dimethylsiloxane) bioreactors during cell culture. *Biomedical microdevices*, *9*(2), 123–34. doi:10.1007/s10544-006-9005-7

Mugnai, S., & Mancuso, S. (2010). Oxygen Transport in the Sapwood of Trees. In S. Mancuso & S. Shabala (Eds.), *Waterlogging Signalling and Tolerance in Plants* (pp. 61–75). Springer Berlin Heidelberg. doi:10.1007/978-3-642-10305-6_4

Nevares, I., Crespo, R., González, C., & del Alamo-Sanza, M. (2014). Imaging of oxygen permeation in the oak wood of wine barrels using optical sensors and a colour camera. *Australian Journal of Grape and Wine Research*, *20*(3), 353–360.

Nevares, I., & del Alamo-Sanza, M. (2015). Oak Stave Oxygen Permeation: A New Tool To Make Barrels with Different Wine Oxygenation Potentials. *Journal of Agricultural and Food Chemistry*, *63*(4), 1268–1275. doi:10.1021/jf505360r

Peterson, R. G. (1976). Formation of Reduced Pressure in Barrels During Wine Aging. *American Journal of Enology and Viticulture*, *27*(2), 80–81. http://www.ajevonline.org/cgi/content/abstract/27/2/80

Piringer, O. G., & Baner, A. L. (2000). *Plastic packaging materials for food : barrier function, mass transport, quality assurance, and legislation*. Weinheim ; New York: Wiley-VCH. http://www.loc.gov/catdir/description/wiley033/00701414.html

Rosenkilde, A. (2002). *Moisture content profiles and surface phenomena during drying of wood*. KTH-Royal Institute of Technology.

Ruiz de Adana, M., López, L. M., & Sala, J. M. (2005). A Fickian model for calculating wine losses from oak casks depending on conditions in ageing facilities. *Applied Thermal Engineering*, *25*(5-6), 709–718. http://www.sciencedirect.com/science/article/B6V1Y-4DD8DH4-3/2/2dd04f4911ab22994629ce58d97f4611

Ruiz de Adana, S. M. (2002). *Aplicación de la Dinámica de Fluidos Computacional al Control de las mermas de vino en naves de crianza climatizadas. Ingeniería mecánica*. Universidad de La Rioja, La Rioja. Retrieved from http://dialnet.unirioja.es/servlet/tesis?codigo=69

Sorz, J., & Hietz, P. (2006). Gas diffusion through wood: implications for oxygen supply. *Trees - Structure and Function*, *20*(1), 34–41. doi:10.1007/s00468-005-0010-x

Sud, D., Mehta, G., Mehta, K., Linderman, J., Takayama, S., & Mycek, M.-A. (2006). Optical imaging in microfluidic bioreactors enables oxygen monitoring for continuous cell culture. *Journal of biomedical optics*, *11*(5), 050504. doi:10.1117/1.2355665

Ungerbock, B., Charwat, V., Ertl, P., & Mayr, T. (2013). Microfluidic oxygen imaging using integrated optical sensor layers and a color camera. *Lab on a Chip*, *13*(8), 1593–1601. http://dx.doi.org/10.1039/C3LC41315B

Ungerböck, B., Mistlberger, G., Charwat, V., Ertl, P., & Mayr, T. (2010). Oxygen imaging in microfluidic devices with optical sensors applying color cameras. *Procedia Engineering*, *5*(0), 456–459. doi:http://dx.doi.org/10.1016/j.proeng.2010.09.145

Ungerböck, B., Pohar, A., Mayr, T., & Plazl, I. (2013). Online oxygen measurements inside a microreactor with modeling of transport phenomena. *Microfluidics and Nanofluidics*, *14*(3-4), 565–574. doi:10.1007/s10404-012-1074-8

Vivas, N., Debeda, H., Menil, F., Vivas de Gaulejac, N., & Nonier, M. F. (2003). Mise en évidence du passage de l'oxygène au travers des douelles constituant les barriques par l'utilisation d'un dispositif original de mesure de la porosité du bois. Premiers résultats. *Sciences des Aliments*, *23*(5-6), 655–678. doi:10.3166/sda.23.655-678

Tables and Figures

Table 1: Main results for selected liquid-wood contact time parameters

Aging time (days)	J^* ($mol \cdot m^{-2} \cdot s^{-1}$)	Oxygen concentration gradient** ($mol \cdot m^{-3}$)	e^{***} (m)	Average (%) MC < FSP	D^{****} ($m^2 \cdot s^{-1}$)	eMC^{*****} (m.%)
6	4.18×10^{-7}	6.18×10^{-6}	3.2×10^{-4}	3.00	2.17×10^{-5}	0.96
13	2.00×10^{-7}	4.63×10^{-5}	5.7×10^{-4}	5.50	2.46×10^{-6}	3.14

20	1.47×10^{-7}	4.63×10^{-5}	5.0×10^{-4}	14.25	1.59×10^{-6}	7.13
32	5.37×10^{-8}	4.63×10^{-5}	6.0×10^{-4}	17.50	6.95×10^{-7}	10.50
63	1.69×10^{-8}	5.87×10^{-4}	5.7×10^{-4}	21.00	1.64×10^{-7}	119.70
88	3.59×10^{-9}	8.49×10^{-4}	6.2×10^{-3}	23.00	2.62×10^{-8}	142.60
125	1.16×10^{-9}	1.00×10^{-3}	7.6×10^{-3}	25.00	8.78×10^{-9}	190.00

* *J* (Diffusion flux) was determined from the evaluation of the OTR of wood at different times in test A.

** Obtained from oxygen imaging analysis (test C) for the thickness where MC > FSP (test B).

*** *e* (Thickness MC > FSP) was obtained from the moisture profile of the wood by the slicing technique (test B).

**** *D* (Oxygen diffusion coefficient) was determined with data from tests A, B and C.

***** *eMC* is the product of the thickness of the flooded layer (*e*) and its average % MC, representing the free water present in that thickness (test B).

Figure 1: Design of experiment with the three different assays carried out: test A, the flow of oxygen that crosses the wood J ($mol \cdot m^{-2} \cdot s^{-1}$), test B, the MC inside the stave (% MC) was obtained at each of the times, and in test C, oxygen concentration profile within the wood.

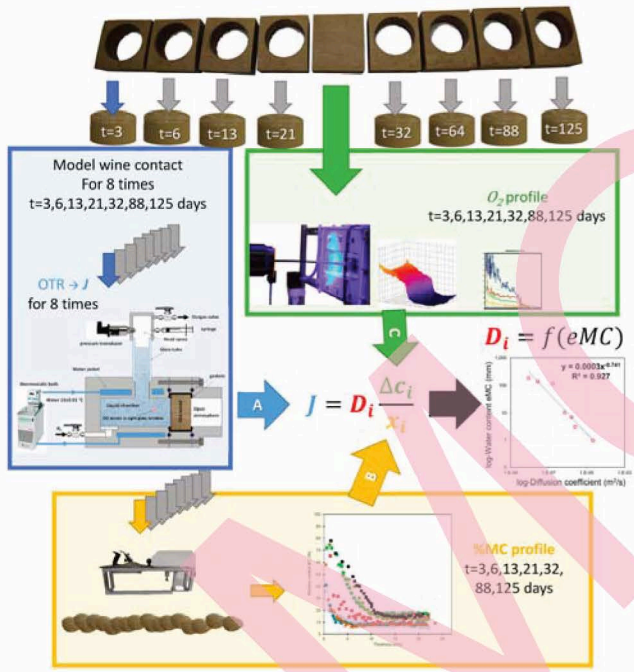

Figure 2: a) calibration curve; compressed air and N_2, b) calibration curve; 2 % O_2 and N_2, c) Referenced image N_2 saturation and d) Referenced image air saturation.

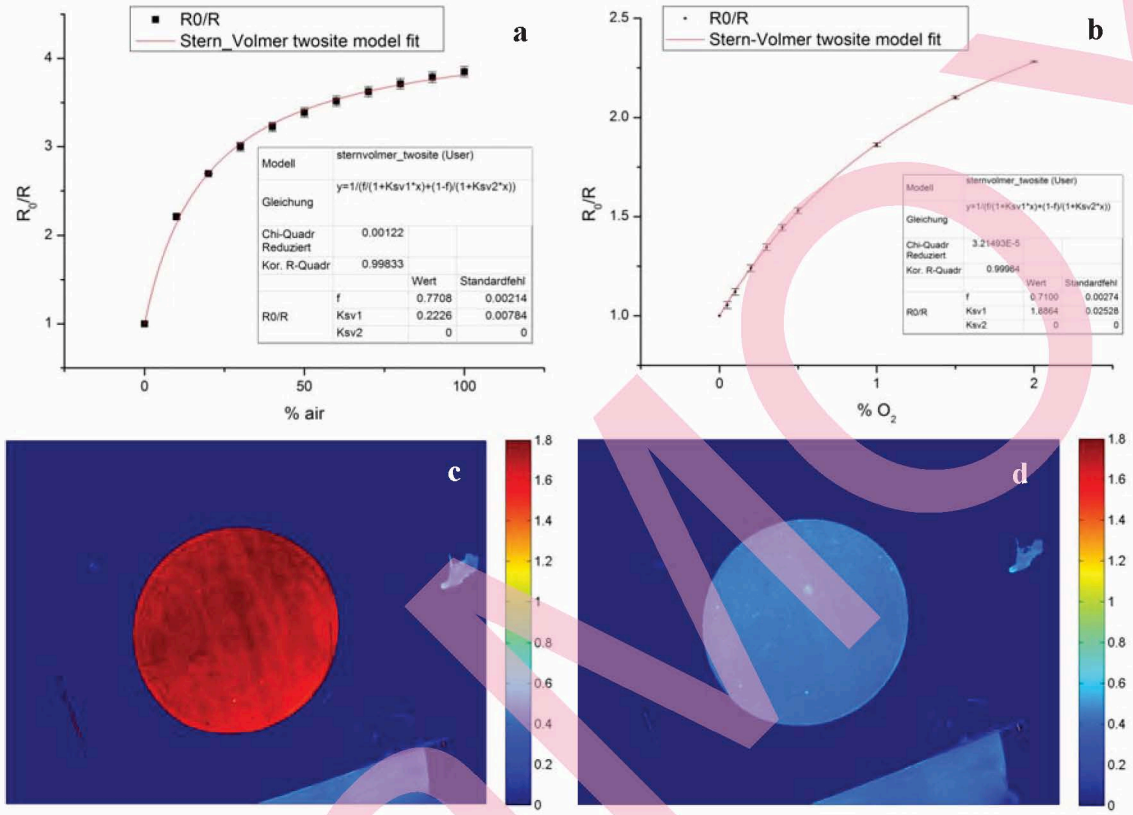

Figure 3: Progression of % MC profiles of oak barrel staves in contact with model wine on one face. The horizontal line represents the FSP, above which free water can be found in the wood.

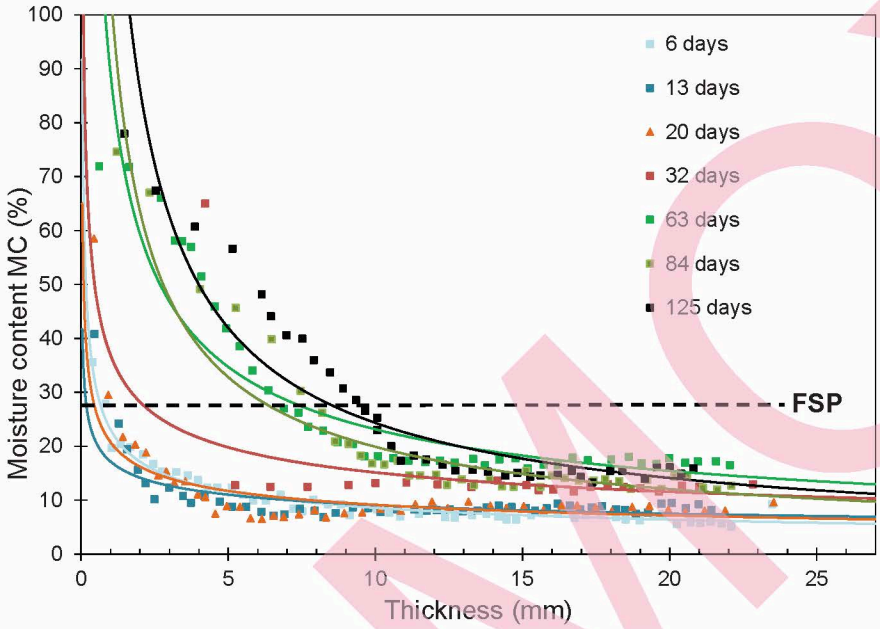

Figure 4: Progression of the diffusion flux J (mol·m^{-2}·s^{-1}), which was obtained from the measurement of OTR in test A with aging time (days) and with adjustment of the potential equation described in previous studies [4]. Relationship of the oxygen diffusion flux J, as calculated with data obtained from test A, with the thickness of the stave wood containing free water (test B).

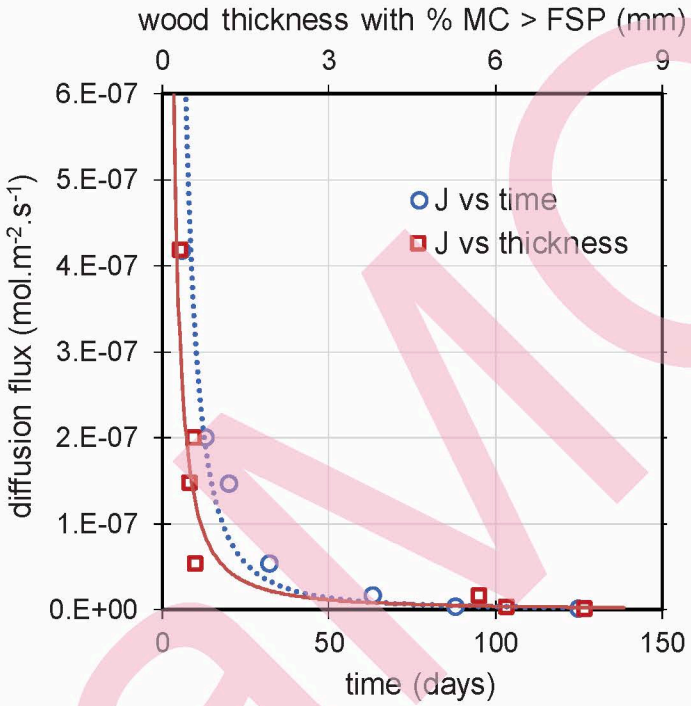

Figure 5. Profiles of the average oxygen concentrations in the thickness of the stave and DO mapping of a section of the stave and the wine in contact with the wood during the 125 days measured, test C.

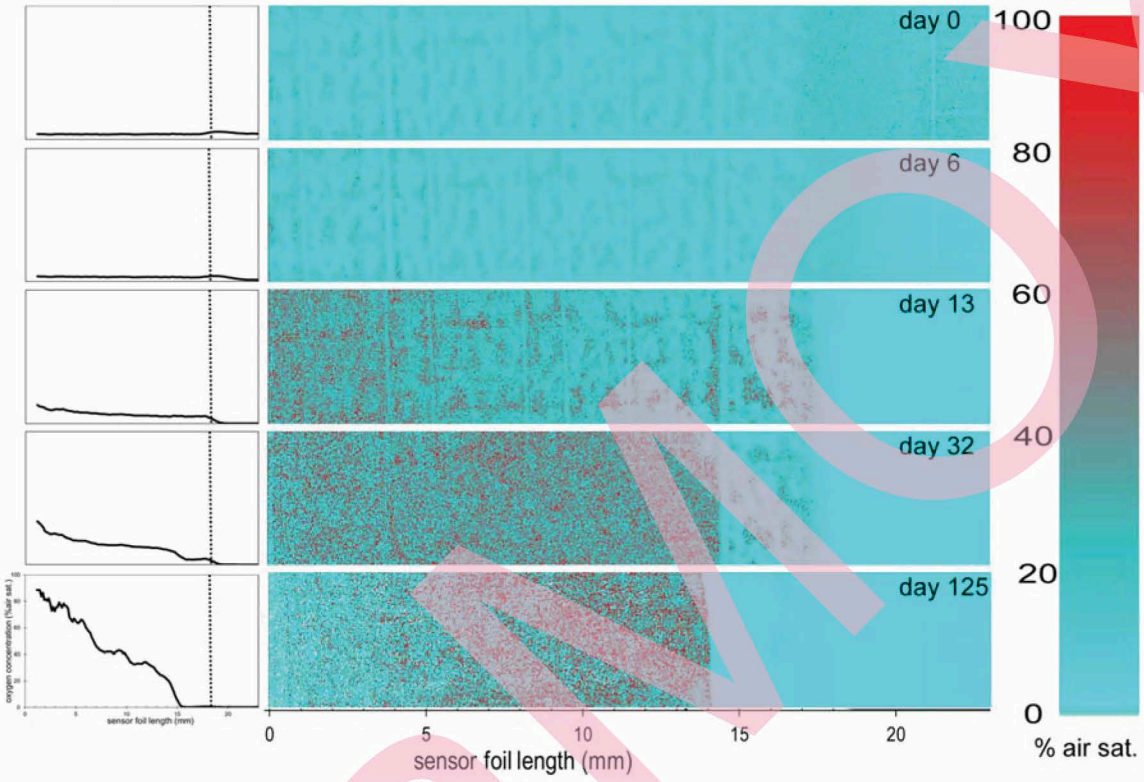

Figure 6. Profiles of the average oxygen concentrations in the thickness of the stave and in the wine in contact with the wood during the 18 weeks measured. Right panel, expansion of the air-wine interface outside and within the stave, from test C.

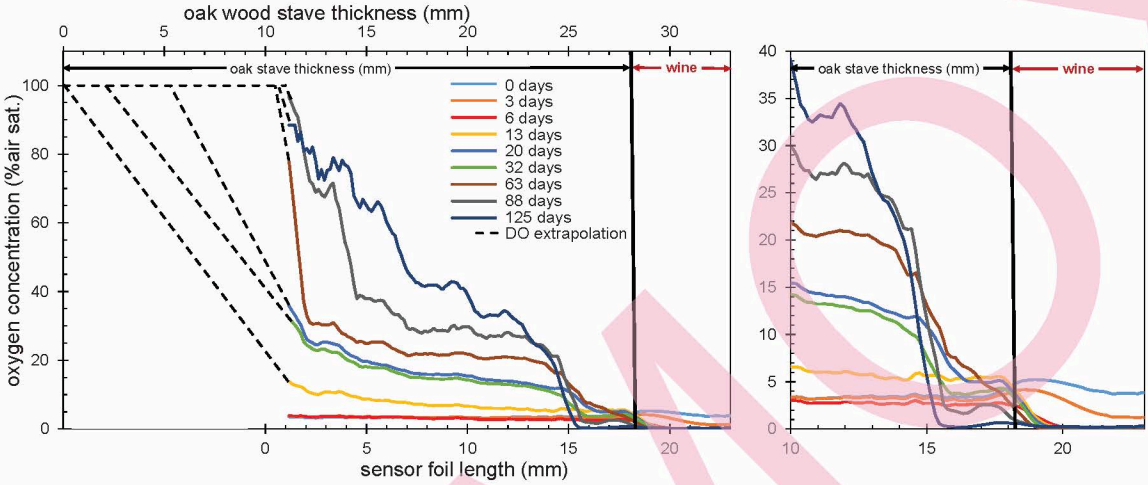

Figure 7. Progression of the oxygen concentration profile (% air sat.) (unbroken line) and the % MC profile of wood (dashed line) at 1, 2, 9 and 18 weeks (test B).

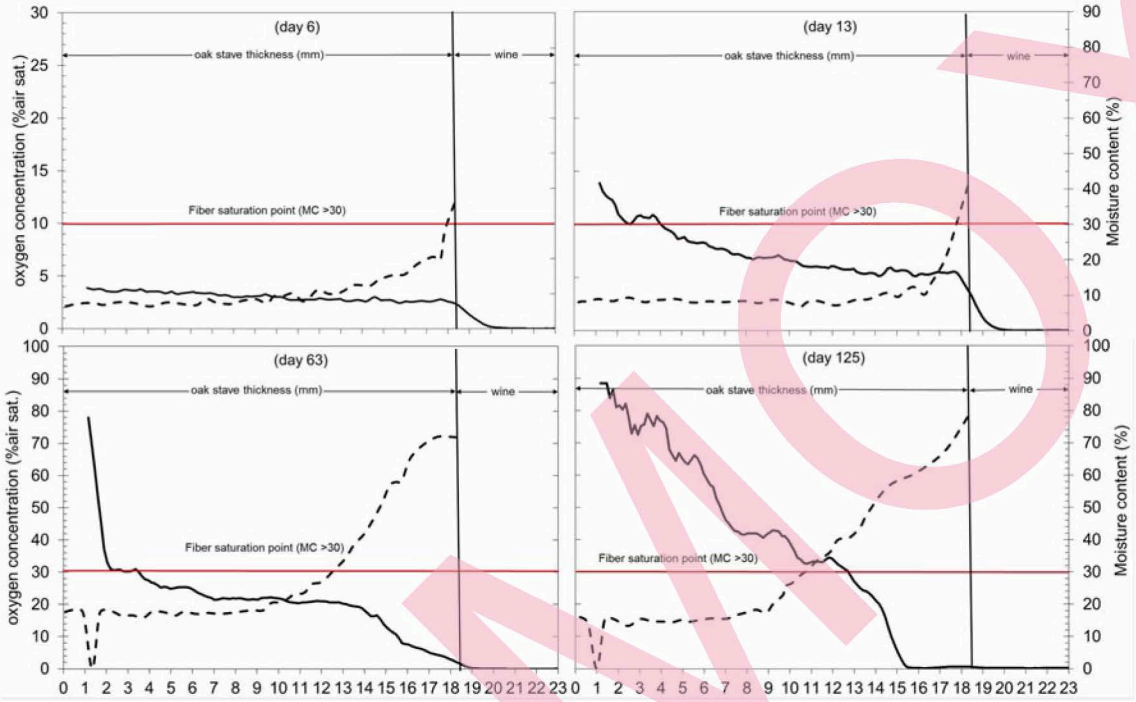

Figure 8. Relationship of the oxygen diffusion coefficient (tests A, B and C) with the thickness of the stave wood containing free water and the amount of water in the flooded layer of the stave in contact with the wine (test C).